

Supporting Information

Optimization and kinetics of crown ether-based hydroxyl-rich organic polymers for sustainable CO₂ fixation and iodine vapor adsorption

Ningning Li¹, Yuhang Zhang¹, Xuanbo Liu¹, Xionglei Wang¹, Yongjing Hao^{1,2},
Tao Chang^{1,2,*}, Zheng Zhu^{1,*}, Balaji Panchal¹, Shenjun Qin^{1,*}

Experimental

Materials and reagents

Dibenzo-18-crown-6, hexamethylenetetramine, trifluoroacetic acid, dichloromethane, KI, HCl (1 mol·L⁻¹), Sodium sulfate, iodine, 1,4-Dioxane, HOAc, hydroquinone, m-benzenetriol, bisphenol A and iodine were purchased from Aladdin Chemical Reagents Co. Ltd. All epoxides contained epichlorohydrin, epibromohydrin, allyl glycidyl ether, phenyl glycidyl ether, butyl glycidyl ether, epoxy hexane and styrene oxide were purchased from Energy Chemical Reagents Co. Ltd. All chemicals were analytical grade and were unpurified. CO₂ at 99.9% purity was supplied by Handan Anke Factory.

Characterization method of material

The FT-IR spectra were measured on a Nicolet IS10 spectrometer (400–4000 cm⁻¹). ¹H NMR spectra were taken on a Bruker 400 spectrometer, and the deuterated chloroform (CDCl₃) with tetramethylsilane (TMS) was used for the internal standard. The ¹³C CP MAS NMR spectrum was acquired on a JNM-ECZ600R spectrometer, the ¹³C chemical shift was related to HMB (hexamethylbenzene). The XPS spectrums were recorded by Thermo Fisher Scientific K-Alpha spectrometer using Al K Alpha source, the pass energy is 150.0 eV and corrected using C1s peak at 284.8 eV. SEM was performed

using a Hitachi SU-8020 microscope with an acceleration voltage of 3.0 kV. Nitrogen adsorption isotherm was achieved from a Micromeritics ASAP 2460 at 77 K, and the sample was degassed at 100°C for 6 h prior to adsorption measurement. Thermogravimetric (TG) curves were gained from STA499. CO₂ adsorption capacity was obtained from a Mike TriStar II Plus 3030 at 273 K, and the polymer was degassed at 120°C for 6 h. The profile of CO₂-TPD was recorded for samples raised from 25°C to 250°C at a rate of 5°C/min and then held at 250°C for 1 h, also using a TriStar II Plus 3030.

Table S1 BET surface area and pore volume of **CHOP@KI-1**

catalysts	Surface area (m ² /g)	Pore volume (cm ³ /g)	Pore diameter (nm)
CHOP@KI-1	5.1601	0.011377	9.4297

Table S2 I⁻ concentration of **CHOP@KIs**

Entry	Catalysts	I ⁻ concentration (mmol/g) ^a
1	CHOP@KI-1	1.0532
2	CHOP@KI-2	0.7941
3	CHOP@KI-3	1.3876

^a checked by ICP-OES.

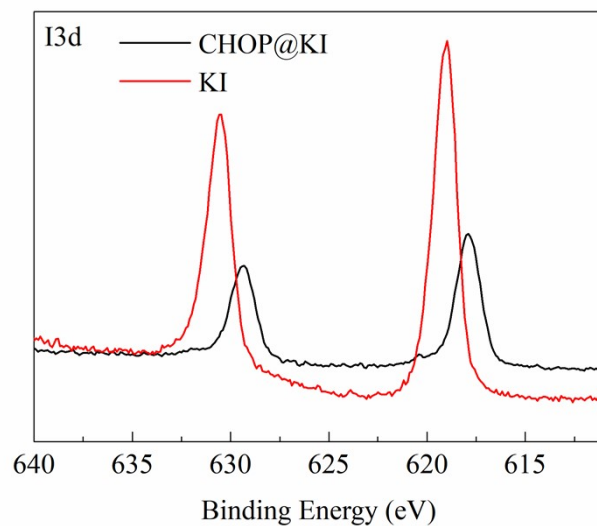


Fig. S1 Interaction of CHOP with KI identified by XPS

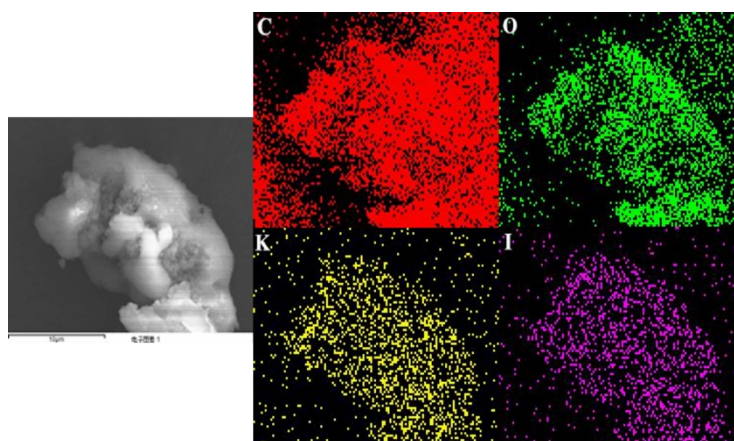


Fig. S2 The C, O, I and K elemental map images of CHOP@KI-1.

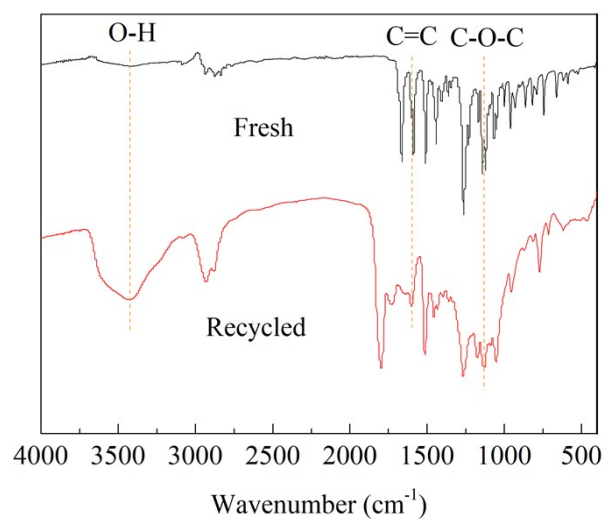


Fig. S3 FT-IR spectra of fresh and recycled catalyst

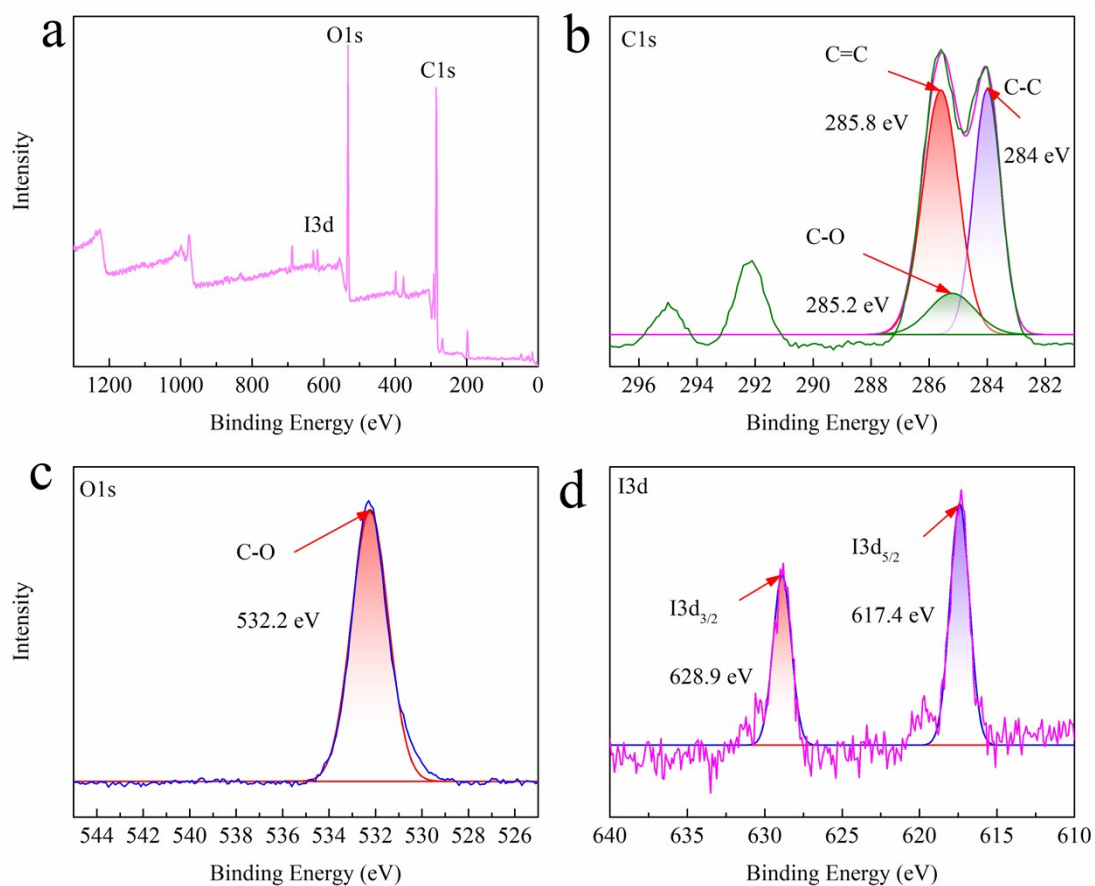


Fig. S4 XPS spectra of recovered CHOP@KI-1, (a) full spectrum, (b) C1s, (c) O1s, (d) I3d.

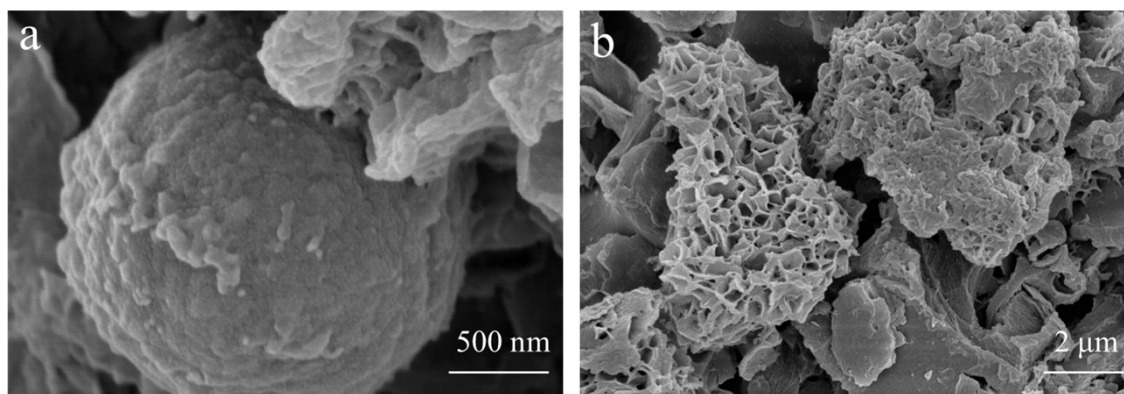


Fig. S5 SEM images of recovered CHOP@KI-1

Kinetic investigations

Table S3 Effects of reaction time by CHOP@KI-1 at 50°C^a

Entry	Time (h)	Yield (%) ^b	1-x	ln(1-x)
1	11	16.20	0.838	-0.176737179
2	13.5	20.40	0.796	-0.228156093
3	16	24.70	0.753	-0.283690051
4	18.5	28.80	0.712	-0.339677368

5 21 33.20 0.668 -0.403467105

a: Reaction conditions: Catalyst: 40 mg, ECH: 10 mmol, solvent-free, 1 atm, T = 60°C; b: detected by ¹H-NMR

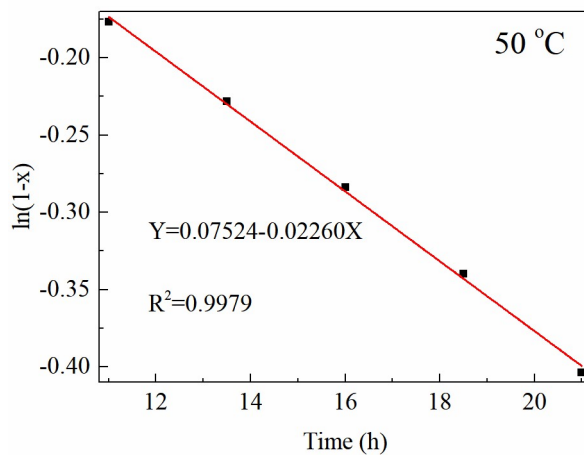


Fig. S6 Ln(1 – x) versus time by **CHOP@KI-1** system at 50°C

Table S4 Effects of reaction time by **CHOP@KI-1** at 60°C^a

Entry	Time (h)	Yield (%) ^b	1-x	ln(1-x)
1	8	16.00	0.84	-0.174353387
2	11	26.70	0.733	-0.310609577
3	14	34.40	0.656	-0.42159449
4	17	41.80	0.582	-0.541284831
5	20	48.70	0.513	-0.667479434

a: Reaction conditions: Catalyst: 40 mg, ECH: 10 mmol, solvent-free, 1 atm, T = 60°C;

b: detected by ¹H-NMR

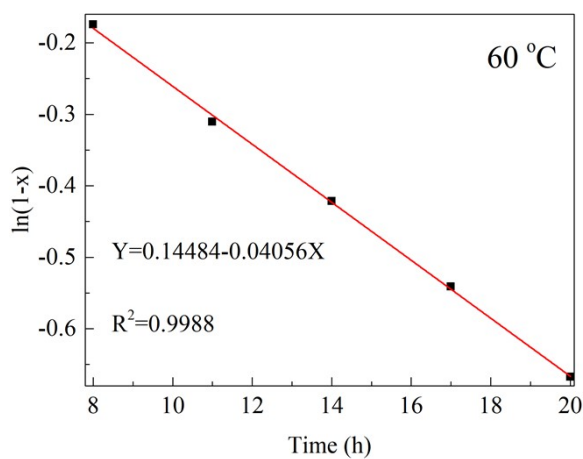


Fig. S7 $\ln(1 - x)$ versus time by **CHOP@KI-1** system at 60°C

Table S5 Effects of reaction time by **CHOP@KI-1** at 70°C^a

Entry	Time (h)	Yield (%) ^b	1-x	$\ln(1-x)$
1	2.5	10	0.9	-0.105360516
2	5	26.30	0.737	-0.305167387
3	7.5	35.10	0.649	-0.432322562
4	10	49.00	0.51	-0.673344553
5	12.5	55.00	0.45	-0.798507696

a: Reaction conditions: Catalyst: 40 mg, ECH: 10 mmol, solvent-free, 1 atm, T = 70°C;

b: detected by ¹H-NMR

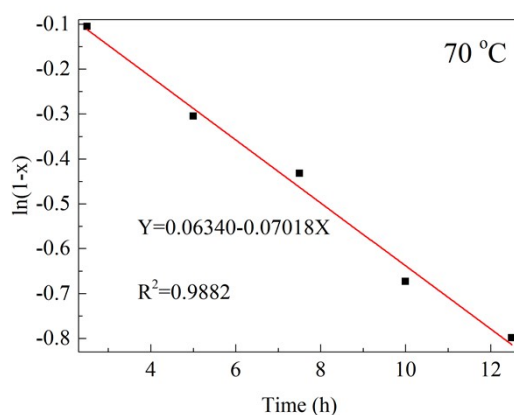


Fig. S8 $\ln(1 - x)$ versus time by **CHOP@KI-1** system at 70°C

Table S6 Effects of reaction time by **CHOP@KI-1** at 80°C^a

Entry	Time (h)	Yield (%) ^b	1-x	$\ln(1-x)$
1	2.5	11	0.888	-0.118783536
2	5	32.60	0.674	-0.394525168
3	7.5	50	0.497	-0.699165253
4	10	68	0.32	-1.139434283
5	12.5	77.00	0.23	-1.46967597

a: Reaction conditions: Catalyst: 40 mg, ECH: 10 mmol, solvent-free, 1 atm, T = 80°C;

b: detected by ¹H-NMR

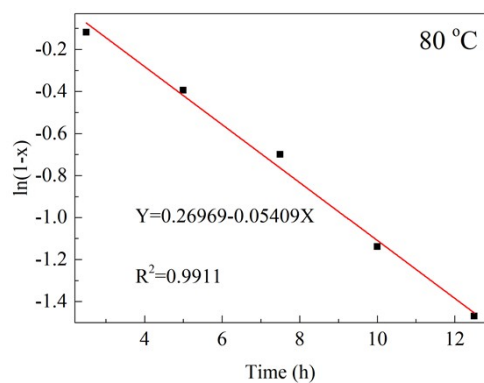


Fig. S9 Ln(1 – x) versus time by **CHOP@KI-1** system at 80°C

Table S7 Effects of reaction temperature on k by **CHOP@KI-1**

Entry	k	ln k	T	1/T
1	0.0226	-3.789805373	323	0.003095975
2	0.04056	-3.20497292	333	0.003003003
3	0.07018	-2.656691909	343	0.002915452
4	0.13787	-1.981444067	353	0.002832861

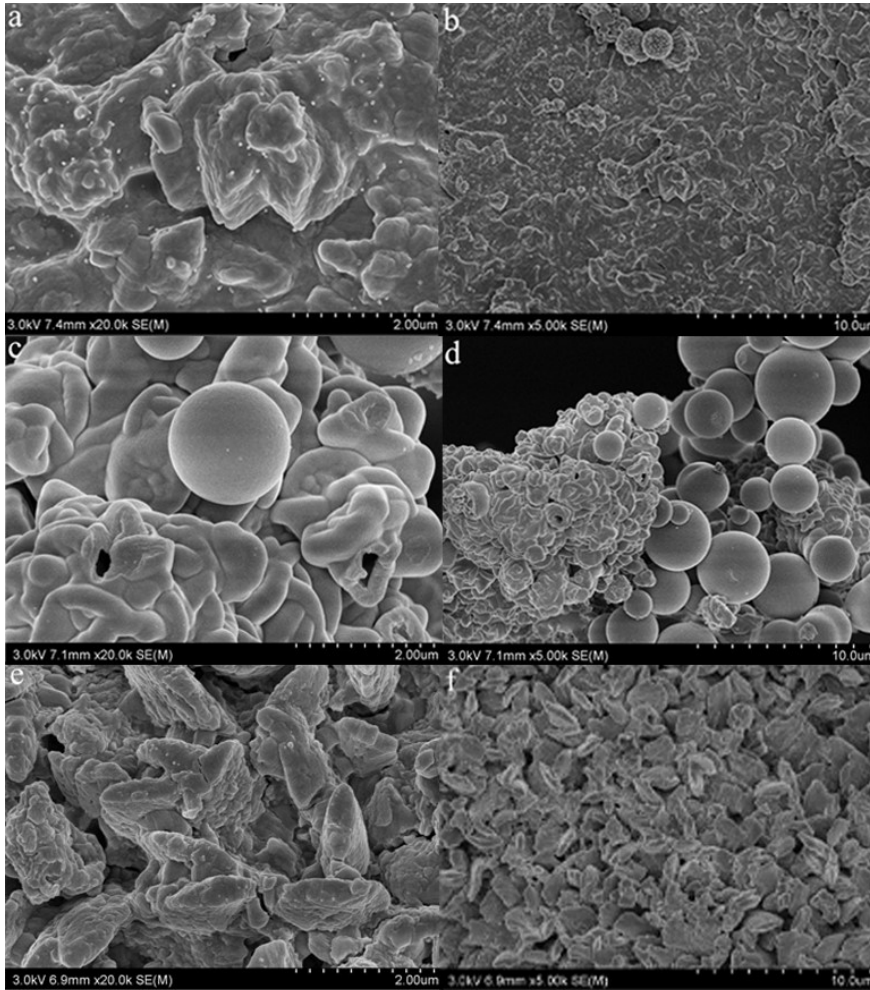


Fig. S10 SEM image of saturated iodine adsorbed by CHOP@KIs

The pseudo-first-order, pseudo-second-order, Boyd's film diffusion and Webber's intraparticle diffusion kinetic models equation as follows:

$$\text{pseudo-first-order: } q_t = q_e(1 - e^{-k_1 t}) \quad (\text{S1})$$

$$\text{pseudo-second order: } q_t = \frac{q_e^2 k_2 t}{1 + q_e k_2 t} \quad (\text{S2})$$

$$\text{Boyd's film diffusion: } F = \frac{q_t}{q_e} \quad (\text{S3})$$

$$\text{For } F \text{ values} > 0.85, Bt = -0.4977 - \ln(1 - F) \quad (\text{S4})$$

For F values < 0.85,

$$Bt = \left(\sqrt{\pi} - \sqrt{\pi - \left(\frac{\pi^2 F}{3} \right)} \right)^2 \quad (\text{S5})$$

Webber's intraparticle diffusion: $q_t = k_i \sqrt{t} + C \quad (\text{S6})$

Where q_t (g g^{-1}) and q_e (g g^{-1}) represent the amount of adsorption captured at time t and at equilibrium time. k_1 (h^{-1}), k_2 ($\text{g g}^{-1} \text{h}^{-1}$) and k_i ($\text{g g}^{-1} \text{h}^{-1/2}$) are the rate constants for pseudo-first-order, pseudo-second-order and Webber's intraparticle diffusion models, respectively. F is the fraction of the equilibrium reached at time t , and Bt is a function of F . C is the intercept of the intraparticle diffusion model.

Table S8. Parameters of pseudo-first-order, pseudo-second-order, Boyd's film diffusion and Webber's intraparticle diffusion models for the adsorption of iodine onto CHOP@KIs.

dynamical model	parameter	CHOP@KI-1	CHOP@KI-2	CHOP@KI-3
pseudo-first-order	$k_1(\text{h}^{-1})$	0.07223	0.05303	0.0622
	$q_e(\text{g} \cdot \text{g}^{-1})$	1.52037	1.48114	1.68203
	R^2	0.99354	0.99444	0.9909
pseudo-second-order	$k_2(\times 10^{-2} \text{g} \cdot \text{g}^{-1} \cdot \text{h}^{-1})$	0.03502	0.02204	0.0246
	$q_e(\text{g} \cdot \text{g}^{-1})$	1.95011	2.01454	2.22728
	R^2	0.97877	0.98677	0.97689
Boyd's film diffusion	Intercept	-0.50511	-0.61274	-0.58573
	R^2	0.95338	0.8869	0.92823
Webber's intraparticle diffusion	$k_{i1}(\text{g} \cdot \text{g}^{-1} \cdot \text{h}^{-1/2})$	0.33098	0.29133	0.36572
	Intercept	-0.28834	-0.319	-0.39951

R^2	0.995	0.99734	0.99772
$k_{i2}(g \cdot g^{-1} \cdot h^{-1/2})$	0.06434	0.1173	0.09224
Intercept	1.01179	0.56053	0.94391
R^2	0.91017	0.98483	0.95254
$k_{i3}(g \cdot g^{-1} \cdot h^{-1/2})$	0.01605	0.01573	0.01563
Intercept	1.35027	1.26227	1.47671
R^2	1	1	1

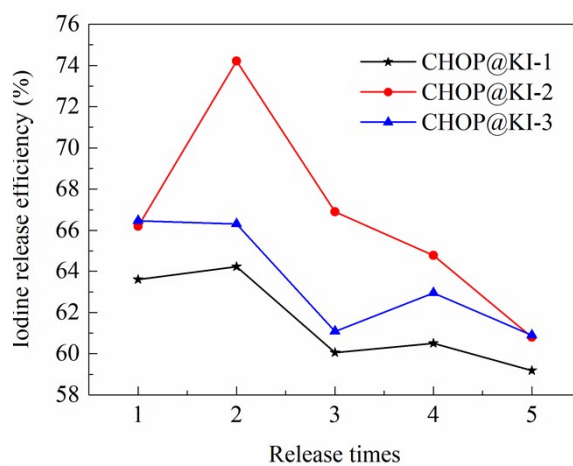


Fig. S11 Iodine release efficiency of saturated samples

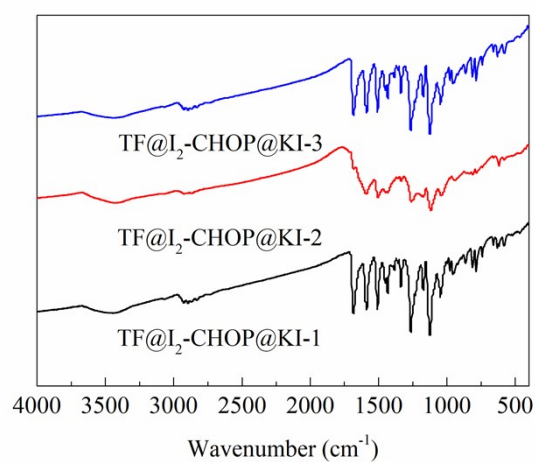


Fig. S12 FT-IR spectra of recycled samples